Title	Nanoscale optical imaging by atomic force infrared microscopy
Authors(s)	Rice, James H.
Publication date	2010-05-01
Publication information	Nanoscale, 2 (5): 660-667
Publisher	RSC Publishing
Item record/more information	http://hdl.handle.net/10197/4463
Publisher's version (DOI)	10.1039/B9NR00279K

Nanoscale IR imaging by combining AFM and optical methodology

James H Rice,
School of Physics, University College Dublin, Belfield, Dublin, Ireland.
Contact email: James.rice@ucd.ie

Abstract

This review outlines an emerging nano-imaging method referred to as Atomic Force Microscopy Infrared Microscopy that enables IR imaging with lateral nanoscale resolution based on combining AFM and optical methodologies. Atomic Force Microscopy Infrared Microscopy enables imaging with nanoscale resolution and enables simultaneously AFM topography imaging. This review outlines the methodology and its application in imaging both biological and functional materials, including an outline of where this emerging method has been applied to image cellular systems in aqueous environments opening up the way for live cell imaging.

1. Introduction

Optical microscopy is an important and widely used method of imaging a range of structures and processes in materials from semiconductors to biological cells. The resolution of optical microscopy has a physical limit, the diffraction limit [1,2]. The maximum resolution in optical microscopy is found to be ca. $\lambda/2$. As a result of diffraction imaging in the infrared using electromagnetic radiation at 5 μm corresponding to an infrared (IR) absorption frequency of 2000 cm^{-1} the image resolution will be 2.5 μm, well above the nanometre length scale). Diffraction means that optical microscopy technology cannot image on the nanoscale (i.e. an image resolution of one hundred nanometres or less), even in the blue region of the visible electromagnetic spectrum [3]. As a consequence the application of optical microscopy to the study of nanoscale functional materials or to emerging disciplines such as nanobiology is limited.

A number of techniques however have been established that does enable imaging of both functional materials and biomaterials and systems on the nanoscale. Important among these are none-optical methods such as electron microscopy, atomic force microscopy (AFM) and X-ray spectroscopy. Electron microscopy techniques such as High-resolution transmission electron microscopy (HRTEM) enables imaging of materials with a resolution better than 1 nm. Electron microscopy is applied to investigate both functional materials and biological processes. This method enables both 2D and 3D imaging when using for example scanning electron microscope based methods [4-6]. While these methods are presently considered state-of-the-art techniques for imaging both functional and biomaterials they possess a imitations in information about the chemical structure of the material under investigation in comparison to what is obtained using optical methods such as Raman or infrared (IR) spectroscopy. X-ray photoelectron spectroscopy, and electrophoretic mobility measurements enables high-resolution studies of cell-surface properties, however these methods require cell manipulation prior to measurements and provide averaged information obtained on ensembles of cells [8,9]. Atomic force

microscopy (AFM) has nm spatial resolution, with the possibility of ambient and live cell imaging [10]. However, while AFM provides detailed topography information, limited information in regard to the chemical composition of the material under inspection can be obtained. Chemical force Microscopy enables AFM to chemical identify surface located species via the use of modified AFM probe tips [11]. While this method is demanding requiring the preparation of AFM tips with specifically chosen organic monolayers it is emerging as an important method to evaluate the chemical composition of in particular biosystems.

Far-field optical microscopy is an envelope that encompasses a large number of different techniques such as Raman, IR, absorption or fluorescence based methods. These methods are based on measuring light that is either transmitted or scattered from the sample, with the light either collected and/or delivered by a microscope objective. Advances in new techniques for sub-diffraction imaging have been made for fluorescence based imaging. A number of fluorescence microscopy techniques have been developed to which overcome this limit in image resolution such as STED and PALM, and are increasingly applied to image both functional materials and biosystems [12]. While these methods are currently among the state-of-the-art methods for sub-diffraction optical imaging in common with other fluorescence methods these methods address specific fluorophore groups and are unable to detect non-luminescent materials present within a host system. To date no advances have been limited for other far-field optical microscopy methods such as Raman and absorption techniques. An alternative method to far-field optical microscopy is near field optical near-field techniques. This method enables imaging with a resolution well beyond the diffraction limit to be obtained. Scanning near-field optical microscopy (SNOM) combines high-resolution scanning probe methods with optical spectroscopy to enable ultrahigh resolution optical microscopy imaging. In SNOM the near-field optical probe is typically 20–120 nm in diameter [13]. This aperture forms the resolution limit which is much smaller than the wavelength of the excitation light, thus providing sub-diffraction limited imaging. The generation of tips with such small apertures is demanding. The probe emits light that consists mostly of evanescent waves instead of propagating waves. As a result of this the incident light interacts with the sample within a layer typical tens of nm from the probe i.e. in the 'near-field' region. This limits significantly the studies that can be performed using SNOM, typically confining this method to surface related studies. In addition, as it is a scanning probe based method, using SNOM to study soft, rough and motile surfaces, such as living cells, is very challenging. However, SNOM has been applied to study a wide range of functional materials and biological systems.

Absorption microscopy has the potential to provide considerable information in regard to the chemical composition of both luminescent and non-luminescent materials [14]. An extensively used form of absorption spectroscopy is infrared absorption (IR) spectroscopy. This method of absorption spectroscopy measures the absorption of light by materials in the infrared region of the electromagnetic (EM) spectrum. IR spectroscopy commonly utilises the region of the EM spectrum between 1.5 – 30 μm (4000 – 400 cm^{-1}). In this region molecular materials absorb radiation via vibration transitions. This enables IR to measure specific frequencies at which constituent parts of molecules corresponding to

specific types of molecular bonds vibrate. This makes possible structural elucidation and compound identification of materials as a consequence IR absorption is extensively used as a (bio)chemical analytical tool. IR absorption spectroscopy when applied to imaging provides a method of chemical imaging or chemical mapping. IR absorption spectroscopy can be achieved using a range of different experimental approaches such as FT-IR, photoacoustic IR, ATR-IR which while they use a range of radiation sources such as free electron laser based sources, OPO lasers, dye lasers or blackbody radiation [15-17]. However, to date these approaches when applied to IR imaging, the lateral spatial resolution (in the X and Y Cartesian axis's) is limited by diffraction to c.a. $\lambda/2$, for IR absorption imaging this results in a spatial resolution on the micron length scale (>1 μm). This has limited the application of IR imaging.

In this review an emerging method referred to as AFMIR that enables IR imaging with lateral nanoscale resolution based on combining AFM and optical methodologies is outlined.

2. Infrared absorption imaging based on combining Atomic force microscopy and optical techniques

Atomic force Microscopy (AFM) enables topographic images of surfaces with very high spatial resolution, i.e. <10 nm [18]. Scattering near-field microscopy (SNIM) is based on the detection of scattered light from an oscillating antenna i.e. an AFM cantilever tip to enable optical imaging with high lateral resolution [19-25]. This method uses a vibrating metallic AFM cantilever tip, which periodically and locally modifies the electromagnetic field distribution of the excitation laser which has been focused to a diffraction limited spot size. SNIM however recover a optical resolution better than the diffraction limit. In addition SNIM simultaneously generates a reflection-mode near-field optical image and a tapping-mode AFM image enabling the sample to be studied mapped independently by topography and optical methodologies.

SNIM can achieve a spatial resolution of $\lambda/100$. SNIM in the infrared has been applied to study heterogeneous sample surfaces under ambient conditions. Several soft and hard condensed matter systems have been studied, including cells and tissues. For example SNIM has been demonstrated wavelength region near 6 μm covered by a line-tuneable CO laser to obtain a lateral resolution of <20 nm [22]. This approach has been use to obtain infrared spectra of single individual poly(methyl methacrylate) nanobeads and viruses at nanoscale resolution (i.e. a lateral resolution of <20 nm). However, due to factors such as the elastic light scattering mechanism and the complex dielectric value of the sample SNIM absorption measurements are approximations of optical absorption measurements [19]. Albeit with this limitation in recovering IR absorption information, SNIM IR imaging has been applied to image a number of systems with a spatial resolution of tens of nm [22]. SNIM has been applied to image functional materials such as insulator-to-metal transition in vanadium dioxide thin films [23]. This studied probed directly percolative insulator metal transition with temperature. In addition to studying biological and functional inorganic materials SNIM has been applied to image functional organic systems such as microstructured self-assembled monolayers, imaging with a lateral resolution of 90 nm

[24]. The authors estimated that this method could chemical image 27 attogram or 30,000 molecules. However, this method collects the scattered light in the far-field and is challenged by low signal intensity. This method is been continuously developed, an example of this is work on evaluating the efficiency of back-scattering based SNIM using a standard cantilevered AFM probe contacting a flat sample and by applying a coherent frequency-comb Fourier-transform method [25].

A separate method to SNIM which also combines AFM and optical methodshas been developed, referred to as Photothermal IR microscopy. Hammiche et al demonstrated that IR spectra of analytes and thin films could be recorded by combining a Fourier transform infra-red spectroscopy instrument with an AFM, a technique referred to as photothermal IR microscopy [23,24]. This approach is based on an opto-thermal method that utilizes specific AFM probes as temperature sensors enabling measurements of opto-thermal signals induced by absorption of IR radiation enabling in turn measurements of IR absorption [25,26]. Photothermal IR microscopy does not require that the AFM tip be in contact with the sample surface but detects heavily damped heat waves generated in the layer of air in contact with the sample surface following irradiation of the sample which leads to absorbed energy dissipated as heat. This method has been applied to image a number of biological systems. Building on this work Dazzie et al demonstrated a method of IR microscopy (referred to as Atomic Force Microscopy Infrared Microscopy or AFMIR) that enables IR imaging with sub-wavelength lateral resolution. AFMIR combines optics and AFM. IR imaging occurs by using the AFM cantilever as the optical detector enabling high resolution imaging [27,28]. This method measures IR absorption directly via measuring local transient deformation in the AFM cantilever induced by an infrared pulsed laser tuned at a vibrational absorbing wavelength (as outlined below). As a consequence, this method is related to photothermal IR microscopy. AFMIR enables IR imaging and simultaneous AFM topography with a spatial resolution on the nanoscale. This review will now concentrate on outlining in detail AFMIR and its applications to date.

2. Atomic Force Microscopy Infrared Microscopy (AFMIR)

2.1. AFMIR's detection mechanism

AFMIR measures directly IR absorption with nanoscale laterial resolution by using an AFM cantilever as the optical detector. AFMIR does this in the following way. The AFM cantilever tip is positioned over the sample with the tip in contact with the sample surface. Following the application of the IR radiation source the cantilever response is monitored, specific a change in vertical displacement of the tip following irradiation of the sample (see Fig 1). This displacement arises from absorption of the incident radiation. Following absorption of the incident radiation, the sample disperses the absorbed energy via thermal and acoustic mechanisms. Propagating acoustic shock fronts induce a vertical displacement of the AFM tip. Measurement of the tip displacement intensity as a function of wavelength enables absorption measurements and absorption imaging. As the incident laser excitation wavelength is tuned into resonance with an absorption transitions of the sample (such as the C-H stretch at c.a. 3.5μm) the displacement intensity increases as it reaches the maximum of the absorption transition, thereafter it will reduce as the excitation wavelength is tuned passed the maximum of absorption. In this way absorption

measurements can be made with high spatial resolution beyond the diffraction limit. Recording the intensity of the cantilever displacement at a fixed time enables intensity to be recorded as a function of excitation wavelength. This enables local IR spectroscopy to be recorded. IR imaging then is performed by monitoring the cantilever intensity as a function of AFM tip position as well as a function of excitation wavelength, in this way IR imaging can be performed. Thus at the heart of the detection mechanism is an induced vertical displacement of the AFM tip. Dazzi et al demonstrated that in contact mode the cantilever vibration modes enables amplification of very small distortions induced by laser absorption enabling measurements of surface deformation normally too small to be measured [27,28]. The authors demonstrated that the cantilever oscillates at resonant frequencies, which amplitudes can be correlated with local absorption, were this system acts as an amplifier of extremely small motions induced by optical absorption. The rapid vertical displacement of the AFM tip from the surface deformation causes the tip to oscillate or vibrate. This vibration in the AFM tip is measured on time scales that precede the time response of the feedback loop. The AFM is operated in contact mode, with a typical setpoint of the tip between 5 and 10 nN. The type of cantilever can be important. The presence of metallic coatings can effect the degree of laser absorption by the tip which effects the background signal. The spring constant of the cantilever will effect the sensitivity of the measurement system, were it is anticipated that a small spring constant is desired as this will enable smaller absorption intensties to be measured potentially. Through analysis of the force curve of the contact and by establishing the set-point, the AFM can remain in a linear range in contact with the surface. AFM topography and IR images are recorded simultaneously which enables two different data sets to be collected and superimposed together to provide information on chemical composition and surface profile.

2.2. Experimental methodology

Two different experimental methods have been demonstrated for AFMIR. Standard AFMIR utilises attenuated total internal reflection (ATR) and as a consequence is limited to measuring samples of thickness of the order of λ, thicker samples will only allow the evanescent waves to partially propagate through [27,28]. Surface AFMIR referred to here as s-AFMIR uses direct excitation of the sample surface via a top-down excitation arrangement enabling samples of undefined thicknesses to be measured in contract to ATR based AFMIR [29].

2.2.1. Standard AFMIR

The most reported method for AFMIR uses an ATR methodology (see Fig 1). This approach measures samples deposited on a ATR compatible ZnSe prism [27,28]. This avoids heating the AFM tip with the laser spot, and reduces the signal background. Residual absorption is further reduced by coating the tips with a gold layer. Excitation of the sample is performed by evanescent waves enabling samples on the order of λ (i.e. some few microns) in thickness to be studied. AFMIR has been to date performed using short laser pulses in the infrared from a free electron laser (CLIO FEL) or using a CO laser. The advantage of using a FEL source is that wavelengths across the mid and far infrared can be

generated, in contrast to table-top laser sources which do not have such a wide wavelength range available.

2.2.2. Surface AFMIR (s-AFMIR)

A top-town excitation arrangement (hereby referred to as s-AFMIR for clarity) based on an in-house built IR laser source and a commercial Atomic force microscope has been demonstrated (see Fig 1) [29]. Mid-IR radiation was generated using a periodically poled $LiNbO_3$ crystal emitting tuneable IR laser radiation, tuneable over 3.13 to 3.57 μm [30]. The generation of infrared laser light by the OPO occurs through a nonlinear process. The PPLN crystal splits the pump photon frequency into an idler and a signal wave where $h\nu_{pump} = h\nu_{idler} + h\nu_{signal}$. To optimise output power and in doing so remove destructive interference arising from the separate group velocities of the pump, idler and signal photon wavelengths quasi phase matched crystal designs were applied. The IR laser is directed onto the surface of the sample been probed by the AFM tip. In this way direct surface excitation is achieved.

3. Application of AFMIR and s-AFMIR to IR imaging of biological and functional materials

AFMIR has been applied to a number of different systems to date. We shall start by reviewing where AFMIR has been applied to study Biological systems and then where AFMIR has been applied to study functional materials.

3.1. Biological systems: Cells, bacteria and viruses

A study of a single fixed Escherichia coli (E. coli) bacteria deposited onto an ATR prism substrate surface was undertaken [27,28]. Imaging the surface features of a single E. coli simultaneous with AFM topography and IR with a spatial resolution of <100 nm. Localised IR spectra of E. coli were recorded using AFMIR and compared with the spectrum of an assembly of bacteria (measured with a far-field FTICR) which showed the same features. AFMIR was then applied to study Escherichia coli bacteria infected with T5 phage (bacteria virus) [31]. Bacteria E. coli was grown in LB medium to the exponential growth phase and infected by phages, where the virus infection was studied at various stages using AFMIR. Single T5 phages were studied as dried samples at two different wavelengths, at 1650 cm^{-1} (amide I) characterizing the proteins of the capsid and at 1080 cm^{-1}, the maximum absorption of the DNA band. These studies indicated that IR images of a single T5 phages could only be obtained at 1650 cm^{-1}. IR imaging at the amide I band produced poor IR images as proteins constitute only a small fraction of the phage head, which is mainly constituted of DNA, the authors demonstrated that when imaging was performed at 1080 cm^{-1} the IR image is blurred compared to the topography indicating that the phages have been damaged arising from denaturing of the virus following drying leading to DNA breakdown. When the T5 phages were prepared infecting the bacteria IR imaging were performed in resonance with the DNA absorption band in order to detect the presence of the virus as as no denaturing of the virus DNA occurs within the bacteria. Dazzi et al studied three stages of infection. Fig 2 shows AFM topography images that were recorded

of the bacterium along with the corresponding IR images of these three stages of infection. These studies indicated that the virus concentration and location could be identified within the bacteria using AFMIR with a resolution of c.a. 100 nm. The authors noted that single viruses could be identified within the bacteria.

AFMIR has been applied to image live cells. Studies of live Candida albicans fungi cells was performed by Mayet et al [32]. Studies were performed using the ATR excitation alignment. This experimental arrangement reduces IR light propagation into the surrounding water environment which in turn reduces sample heating and thus minimizing sample perturbation. Blastospore and Hyphea candida albicans fungi were studied in water. These systems were studied between 800–1200 cm^{-1} in order to assess the water window. IR imaging was performed at the glycogen band centred at 1080 cm^{-1}. The resulting IR images indicated that the glycogen band is distributed uniformly. Water absorption was shown to occur with significant strength from 900 to 800 cm^{-1}, while relatively low water absorption occurred between 900 to 1200 cm^{-1}. Simultaneous AFM images and IR images were recorded (see Fig 3) enabling cross confirmation of images profiles. Comparing these images showed that the intensity of the glycogen band signal in the IR image matches the AFM topography image profile for each sample studied. These studies demonstrated that the AFM cantilever vibration in water could be measured and IR imaging was possible. Effects arising from the water environment on the measured vibrations from the cantilever were reported but these effects arising from friction forces etc while present did not preclude imaging. The authors showed that through Fourier technique analysis enables the contribution of the sample from the surrounding absorbing medium to be resolved. Studies of water absorption were also made showing that the wavelength window of imaging was required to be carefully chosen in order to avoid strong water absorption transitions. The authors reported that the spatial resolution seems identical in liquid than in air at ca 100 nm. This study demonstrated that live cell imaging can be performed using AFMIR.

3.2. Self assembled quantum dots and inorganic microstructures

The spectral measurement of the absorption of quantum dots has been reported for visible or near-infrared wavelengths in resonance with interband transitions involving electron and hole pairs, however measurements of intraband transitions in single quantum dots is challenging. AFMIR has been successfully applied to measure single quantum dot absorption in the mid-infrared spectral range at room temperature [33]. Houel et al applied AFMIR to study intra-band transitions in single n-doped InAs/GaAs self-assembled quantum dots which were prepared with a 20 nm capping layer. Charged self-assembled quantum dots with electrons (or holes) can undergo inter-sublevel absorption transitions between discrete confined levels which typically occur at mid or far-infrared energies depending on the properties of the quantum dot probed. AFMIR was applied to InAs/GaAs self-assembled quantum dots which were of c.a. 20 nm in width and c.a. 4 nm in height, exhibiting inter-sublevel transitions between 8–20 μm at room temperature. A weak absorption cross-section estimated at $3x10^{-9}$ for a resonant inter-sublevel transition at 10 μm was reported which overlaps with background ambient blackbody radiation. Measurements of intra-sublevel transitions in single quantum dots at 9.6 μm using AFMIR

were undertaken [33]. The authors measured in resonance with intraband transition of a single charge between discrete confined levels originating from the conduction band, specifically the observed absorption was assigned to arise from two *S-D* bound-to-bound intersublevel absorptions. The intensity of these absorptions was recorded as a function of AFM tip position enabling imaging. Mapping of the quantum dots was performed at 9.6 μm with a spatial resolution of λ/150 i.e. 60 nm. Fig 4 shows the AFM topography, AFMIR and theoretical calculations obtained in this study. Fig 4b shows the AFMIR image for a sample with a specific doping concentration were the white colour corresponds to the IR absorption signature of single quantum dots. The authors noted that only a small fraction of the quantum dots can be observed in the image among the c.a. 250 quantum dots statistically buried under the surface. This was suggested to arise from the fact that all the quantum dots are not significantly populated at room temperature as a result of the balance between carrier capture and thermionic emission in addition only a fraction of the quantum dots exhibits absorption spectrally resonant with the laser wavelength (as supported by theoretical calculations outlined in Fig 4 which match with experimental data). Furthermore the authors noted that larger spots in Fig 4b can be seen attributed to a gathered group of several dots which cannot be spatially resolved. Fig 4c shows an AFMIR image of a quantum dot with a reduced charge population, which shows less image features while Fig 7d shows the AFMIR spectrum for a highly charged quantum dot sample showing increased image features. This study demonstrated that imaging with very high lateral spatial resolution (i.e. 60 nm) can be archived with AFMIR. In addition AFMIR can be applied to image sub-surface features with the quantum dots imaged by Houel et al present 20 nm below a semiconductor capping layer [33].

IR bulk GaAs phonon absorption and IR absorption of thin SiO2 microdisks were studied using AFMIR by Houel et al [34]. AFMIR imaging was performed with a laterial spatial resolution achieved with microdisks of around 50 nm. AFMIR imaging followed the spectral dependence of the bulk absorption. The measurements on bulk GaAs and on SiO_2 microdisks deposited on silicon showed that both surface and bulk can contribute to the signal. This was interpreded by the authors to indicate that both the acoustic and thermal propagation of the deformation plays an important role which can lead to phase delays and can induce a decrease of the oscillation amplitude of the cantilever.

3.3. Polymer micostructures

s-AFMIR has been applied by Hill et al to image soft matter systems, specifically micro-polystyrene beads [29]. To date this is the only application of s-AFMIR in the literature. IR absorption and AFM topography images of polystyrene beads were recorded simultaneously with an image resolution of 200 nm. Chemical maps were reported at 3000 cm^{-1} in transition with the C-H stretch of the polystyrene system. Local IR spectroscopy was performed by placing the tip over a polystyrene bead (in contact mode) and scanning the excitation wavelength while keeping the tip stationary. The local spectrum with a spatial resolution of c.a. 200 nm was thus recovered (shown in Fig 5). This spectrum compared well with a FTIR sample of polystyrene film. IR images recorded at the absorption maxima at c.a. 2925 cm^{-1} (position α) and not in resonance with an IR absorption band at 2800 cm^{-1}(position β). Fig. 5. Shows the IR absorption image recorded

at the C–H vibration frequency (position α as outlined in Fig 5d) and away from it (position β as outlined in Fig 5) respectively, plus the AFM topographic image. The IR absorption image recorded on the absorption peak shows an object that absorbs intensely (light colouring) present on a nonabsorbing (dark) background. The position and extent of the IR absorbing object matches the AFM topography image. This study demonstrated that direct surface excitation of the sample enables AFMIR imaging.

4. Discussion and conclusion

A range of methods exist for IR imaging such as Photoacoustic microscopy, synchrotron infrared microspectrometry, however the spatial resolution of these approaches is limited by diffraction to λ/2 [14-17,37-40]. Resulting in the lateral IR image resolution limited to the micron lengthscale. The use of attenuated total internal reflection (ATR) methodology however provides a method to provide enhanced vertical spatial resolution by utilizing evanescent waves to probe samples studying samples on the order of the evanescent waves penetration depth i.e. on the order of lamda [35-36]. ATR does not improve the laterial spatial resolution which is critical for surface imaging in particular.

Alternative methods of vibrational spectroscopy imaging to IR methods exist. Raman microscopy has been able to provide high spatial resolution spectroscopic imaging via the use of small lamda (via using EM radiation in the near-UV) and confocal methodologies, matching the spatial resolution of fluorescence microscopy. While in theory it is possible to continuously improve the spatial resolution of Raman microscopy via the use of higher excitation frequencies into the UV and higher (soft x-ray region etc), it has been found that excitation of materials notable biosystems at such high excitation energies produces fluorescence which ‘drowns’ the Raman signal. This has effectively resulted in the lateral resolution of Raman microscopy been above the nanoscale. In contrast, the spatial resolution of AFMIR is determined ultimately by the AFM cantilever profile. This has enabled imaging with 60 nm lateral resolution (at a wavelength of 10 μm resulting in an image resolution of λ\150). Raman imaging and established IR imaging methods are limited to λ\2 by the Abbe limit. Near-field approaches have been demonstrated that enable IR and Raman spectroscopy imaging to be performed. These approaches utilise optical apertures, plasmon enhancement effects and/or tip oscillations methods to enable imaging. However such approaches do not enable the recovery of IR absorption information which in contrast Raman spectroscopy, been a scattering technique, can berecovered successfully. However, challenges remain with such Raman based methods for example, the optical detector (typically a CCD) is in the far field leading to the Raman signal that is recovered been weak [41].

The application of AFMIR to biological systems has been demonstrated by probing bacterium and living cells (as outlined above). These studies demonstrated that soft matter i.e. biological systems can be probed using AFMIR and significantly that living systems can be studied using this method. It is noted that the presence of water, which is a strong IR absorber limits the spectral window in the IR and a consequence limits the potential of this method to chemical map living biosystems. In contrast to this other spectroscopic imaging methods such as Raman are not so limited by the presence of water and can potentially

probe a wider spectral window. Studies of biosystems to date performed using AFMIR have probed the surface features of both live and fixed cells which have reported homogeneous distribution of specific chemical functional groups, ie. the Amide I band or the glycogen band. However, when probing relatively large features such as viruses within a host organism [31], the power of AFMIR becomes apparent demonstrating that in order to utilise this method to its full potential AFMIR should be applied to systems that have inhomogeneous distributions of material. An second example of this is the study of quantum dot materials embedded within a wider band gap host. Houel et al in their studies of quantum dot materials using AFMIR showed, via probing intra-sub-band transitions, the presence of InAs/GaAs quantum dots within a host system [33].

Present AFMIR technology has been expanded to include to two experimental methodologies, ATR and direct surface excitation, enabling a wide range or samples to be mapped with high lateral resolution. It is noted however, that such mapping is limited in the Z plane. Studies of virus in bacteria demonstrated that viruses present beneath the host surface can be imaged but with undefined resolution [31]. Presently the inability to resolve information in the Z plane is a limit in the imaging ability of AFMIR.

In conclusion, AFMIR enables local spectroscopy or chemical mapping of materials with nanoscale resolution simultaneously with AFM topography imaging with nanoscale spatial resolution. This approach combines atomic force microscopy and an infrared-pulsed laser. This nano-tool has been applied to enable local IR spectroscopy (utilising a stationary AFM tip) or chemical imaging (utilising a scanning AFM tip) of biomaterials, organic polymer systems and semiconductor materials. AFMIR imaging can be made of systems in aqueous environments demonstrating that live cell bio-imaging can be undertaken within the IR water window.

5. References

1. E. Hecht, “Optics”, Addison and Wesley, Reading, MA, 3rd edn, (1998).
2. E. Abbe, Arch. Mikroskop. Anat., 9, 413–420 (1873).
3. S. W. Hell, Nat. Nanotechnol., 21, 1347–1355 (2003).
4. P. Walther , “High Resolution Cryoscanning Electron Microscopy of Biological Samples” in Biological Low-Voltage Scanning Electron Microscopy (2008).
5. R. Egerton, “Physical principles of electron microscopy”. Springer (2005).
6. Y. Shao-Horn, L. Croguennec, C. Delmas, E.C. Nelson, M.A. O’Keefe, Nature Mat. 2, 464-467 (2003).
7. F. Verni, S. Gabrielli, “From Cells to Proteins: Imaging Nature across Dimensions” Vol 3, Springer Netherlands (2006).
8. J. Ubbink, P. Schar-Zammaretti, Micron 36, 293–320 (2005).
9. N. Mozes, P.S. Handley, H.J. Busscher, P.G. Rouxhet, "Microbial Cell Surface Analysis: Structural and Physicochemical Methods", VCH Publishers, New York (1991).
10. B.P. Jena, J.K. Heinrich-Horber, L. Wilson, P.T. Matsudaira, “Atomic Force Microscopy in Cell Biology”, Academic Press London (2002).
11. Y.F. Dufrêne, Nature Protocols, 3, 1132-1138 (2008).
12. J.H. Rice, Molecular BioSystems, 3, 781-793 (2007).

13. B. Hecht, B. Sick, U.P. Wild, V. Deckert, R. Zenobi, O.J.F. Martin, D.W. Dieter, J. Chem. Phys, 112, 7761–7774 (2000).
14. R Lalanne, F. Carmona, L. Servant, "Optical Spectroscopies of Electronic Absorption", World Scientific Publishing Company , New York (1999).
15. A.J. McQuillan, Adv. Mater. 13, 1034-1038 (2001).
16. H.F. Zhang, K. Maslov, G. Stoica, L.V. Wang, Nature Biotechnology 24, 848–851 (2006).
17. K. Nishikida, E. Nishio, R.W. Hannah, "Applications of Modern FT-IR Techniques", Kodanska LTD with Gordan and Breach Publishing, Toyko (1985),
18.T. R. Albrecht, C. F. Quate, J. Vac. Sci. Tech. A., **6**, 271-274 (1988).
19. R. Bachelot, P. Gleyzes, C. Boccara, Optics Lett., 20,1924 (1995)
20. B. Knoll, F. Keilmann, Nature, **399**,134 (1999).
21. S. C. Kehr, M. Cebula, O. Mieth, T. Hartling, J. Seidel, S. Grafstrom, L. M. Eng, S. Winnerl, D. Stehr, M. Helm, Phys., Rev., Lett., **100**, 256403 (2008)
22.19. M. Brehm, T. Taubner, R. Hillenbrand, F. Keilmann, Nano Letts., **6**, 1307 (2006).
23.20. M.M. Qazilbash,1 M. Brehm, G.O. Andreev, A. Frenzel, P.-C. Ho, B-G Chae, B-J Kim, S.J Yun, H.-T. Kim, A.V. Balatsky, O.G. Shpyrko, M.B. Maple, F. Keilmann, D.N. Basov, Phys. Rev. B., **79**, 075107 (2009)
24.21. I. Kopf, J. Sebastien S. Go1tz Wollny, C. Grunwald, E. Bru1ndermann, M. Havenith, J. Phys. Chem. C, **111**, 8166-8171 (2007).
25.22. M. Brehm, A. Schliesser, F. Čajko, I. Tsukerman, F. Keilmann, Optics Express., **16**, 11203 (2008).

23. A. Hammiche, M. H. Pollock, M. Reading, M. Claybourn, P. M. Turner, K. Jewkes, Appl. Spectrosc., **53**, 810-815 (1999).
24. A. Hammiche, L. Bozec, M. J. German, J. M. Chalmers, N. J. Everall, G. Poulter, M. Reading, D. B. Grandy, F. L. Martin, H. M. Pollock, Spectrosc., **19**, 20-24 (2004).
25. A. Hammiche, L. Bozec, H. M. Pollock, M. German, M. Reading, J. Microsc., **213**, 129-134 (2004).
26. M. Reading, D. M. Price, D. B. Grandy, R. M. Smith, L. Bozec, M. Conroy, A. Hammiche, H. M. Pollock, Macromol. Symp., **167**, 45-62 (2001).
27. A. Dazzi, R. Prazeres, F. Glotin, J. M. Ortega, Infr. Phys. Tech., 49, 113-121 (2006).
28. A. Dazzi, R. Prazeres, F. Glotin, J. M. Ortega, Ultramicroscopy, 107, 1194-1200 (2007)
29. G. Hill, J.H. Rice, S.R. Meech, P. Kuo, K. Vodopyanov, M. Reading, Optics Letters, 34, 431–433 (2009).
30. K. L. Vodopyanov, P. G. Schunemann, Opt. Lett., **28**, 441-443 (2003).
31. A. Dazzia, R. Prazeresa, F. Glotina, J.M. Ortegaa, M. Al-Sawaftaha, M. de Frutos, Ultramicroscopy 108 635–641, (2008).
32. 34. C. Mayet, A. Dazzi, R. Prazeres, F. Allot, F. Glotin, J. M. Ortega, Optics Lett., 33, 1611-1614 (2008)
33. J. Houel, S. Sauvage, P. Boucaud,, A. Dazzi, R. Prazeres, F. Glotin, J.-M.Ortega, A. Miard, A. Lemaıtre, Phys. Rev. Lett., 99, 217404 (2007)
34. J. Houel, E. Homeyer, S. Sauvage, P. Boucaud, A. Dazzi, R. Prazeres, J.M.Ortega, Optics Exp., 17, 10887-10894 (2009).
35. L.G. Tisinger, A.J. Sommer Microsc. Microanal., 10(Suppl 2), 1318-1319 (2004).

36. K.L.A. Chan, S.G. Kazarian, Appl. Spec., 61, 48-54 (2007).
37. P. Rullhusen, X. Artru, P. Dhez, Novel Radiation Sources Using Relativistic Electrons: From Infrared to X-rays (Series on Synchrotron Radiation Techniques & Applications), World Scientific Publishing Co Pte Ltd, London (1998).
38. D. Eichert, L. Gregoratti, B. Kaulich, B, A. Marcello, P. Melpignano, L. Quaroni, M. Kiskinova, Analt. Bioanalt. Chem., 389, 1121-1132 (2007).
39. H.U, Gremlich, B. Yan, "Infrared and Raman Spectroscopy of Biological Materials", CRC Press. London (2000).
40. H.H. Mantsch, D. Chapman, "Infrared Spectroscopy of Biomolecules", Wiley Blackwell, London (1996).
41. M. Micic, N. Klymyshyn, Y.D. Suh, J. Phys. Chem., 107, 1574-1584 (2003).

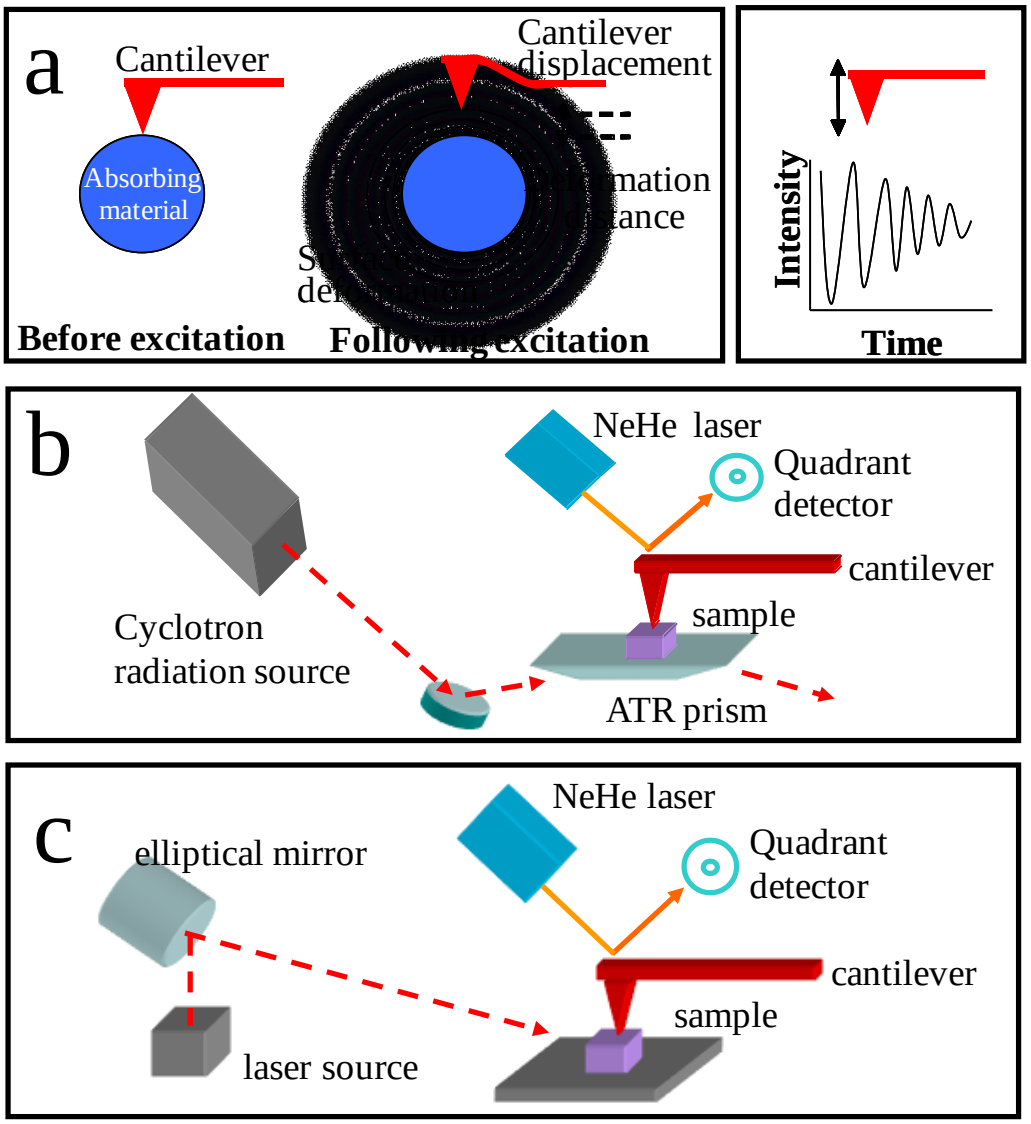

Fig 1. Schematic drawing of a) the cantilever and sample before and after absorption of radiation, shown is the surface deformation effects creating displacement in the position of the cantilever following excitation (left), a graph of the intensity of the resulting cantilever oscillations over time following excitation (right) ,b) the ATR based AFMIR set up which uses a free electron laser, c) top-down experimental set up which uses a table top PPLN based laser system.

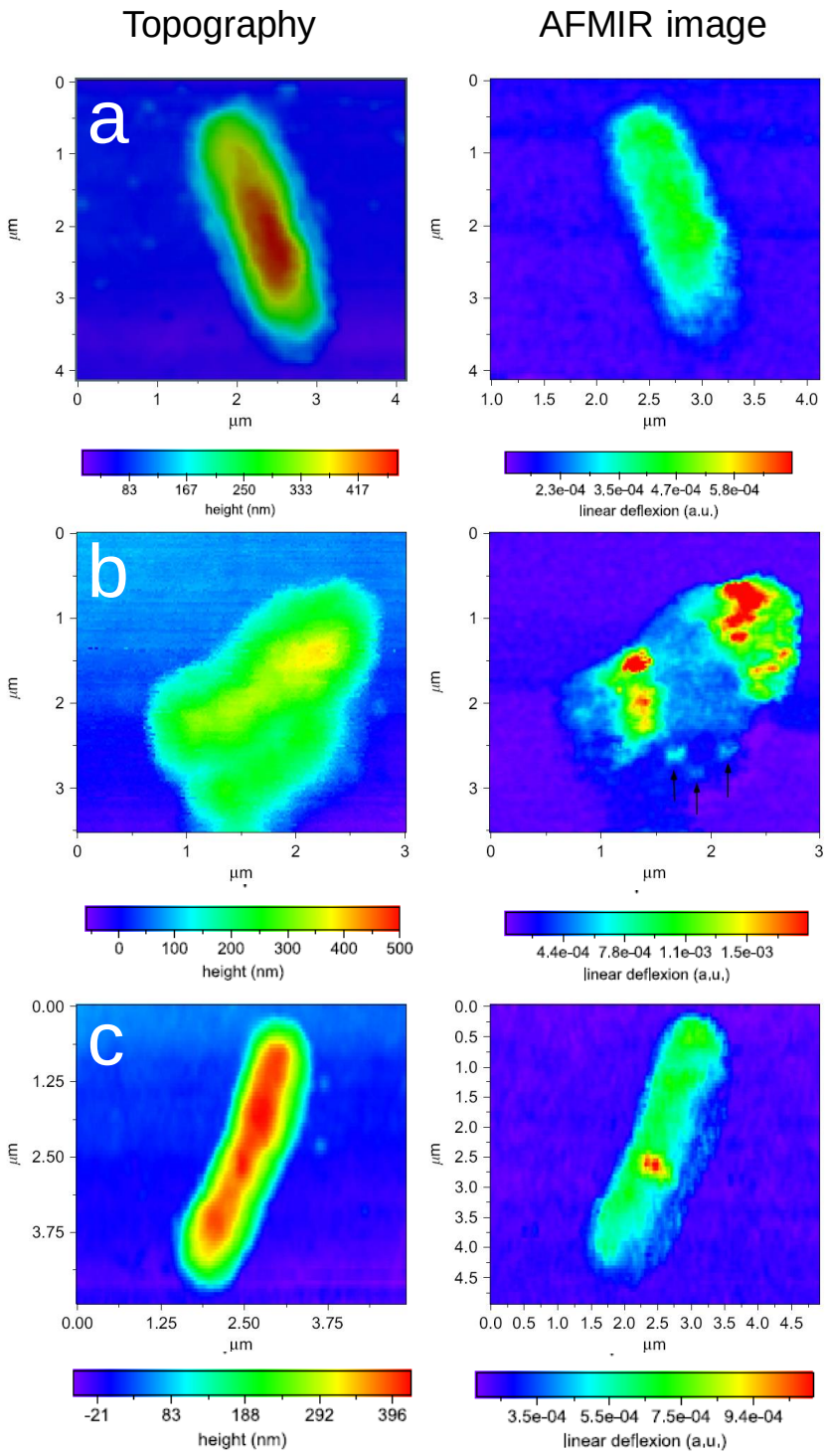

Fig 2. Study of a single Escherichia coli bacteria and T5 phage bacteria virus. AFMIR chemical mapping images recorded at 1080 cm^{-1} of three stages of infection. a) non-infection, b) heavily infected, and c) only one phage visible. [taken from ref 31, copyright Elsevier publishing, reproduced with permission].

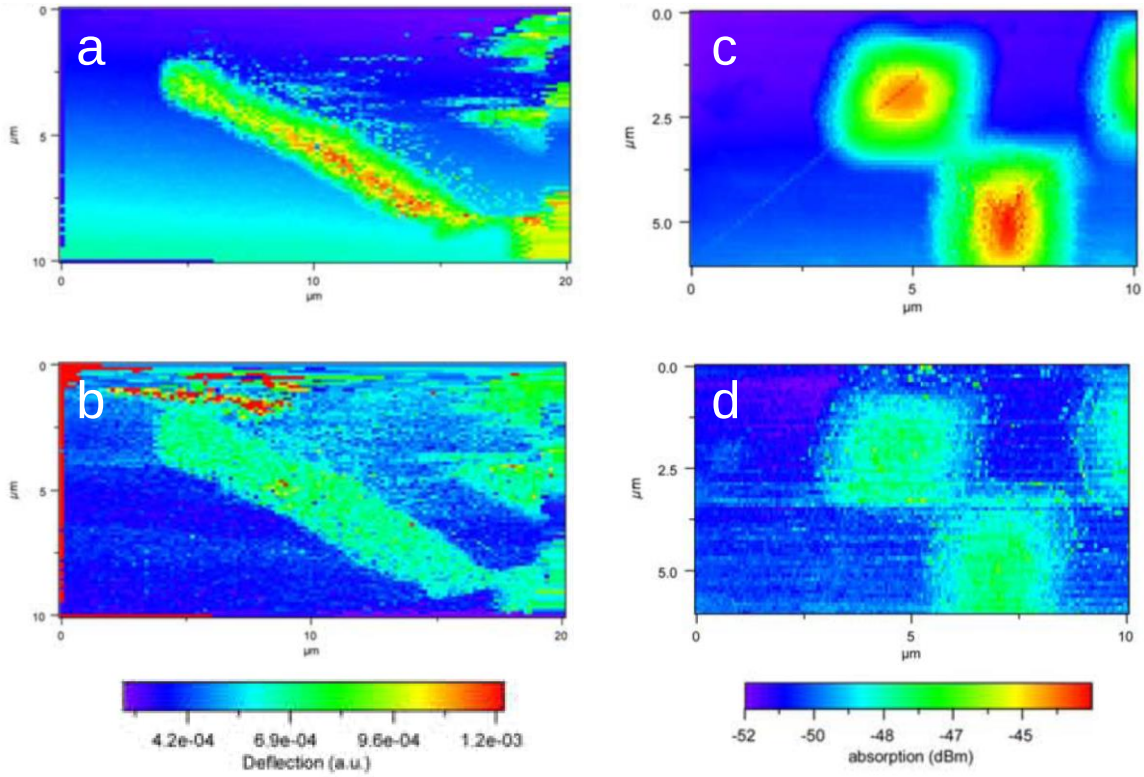

Fig.3. Candida albicans fungi cell left, hyphae and right, blastospore immersed in water. a) and c,) AFM topography; b) and d) AFMIR images at 1080 cm^{-1} [taken from ref 32, copyright Optical Society of America, reproduced with permission]

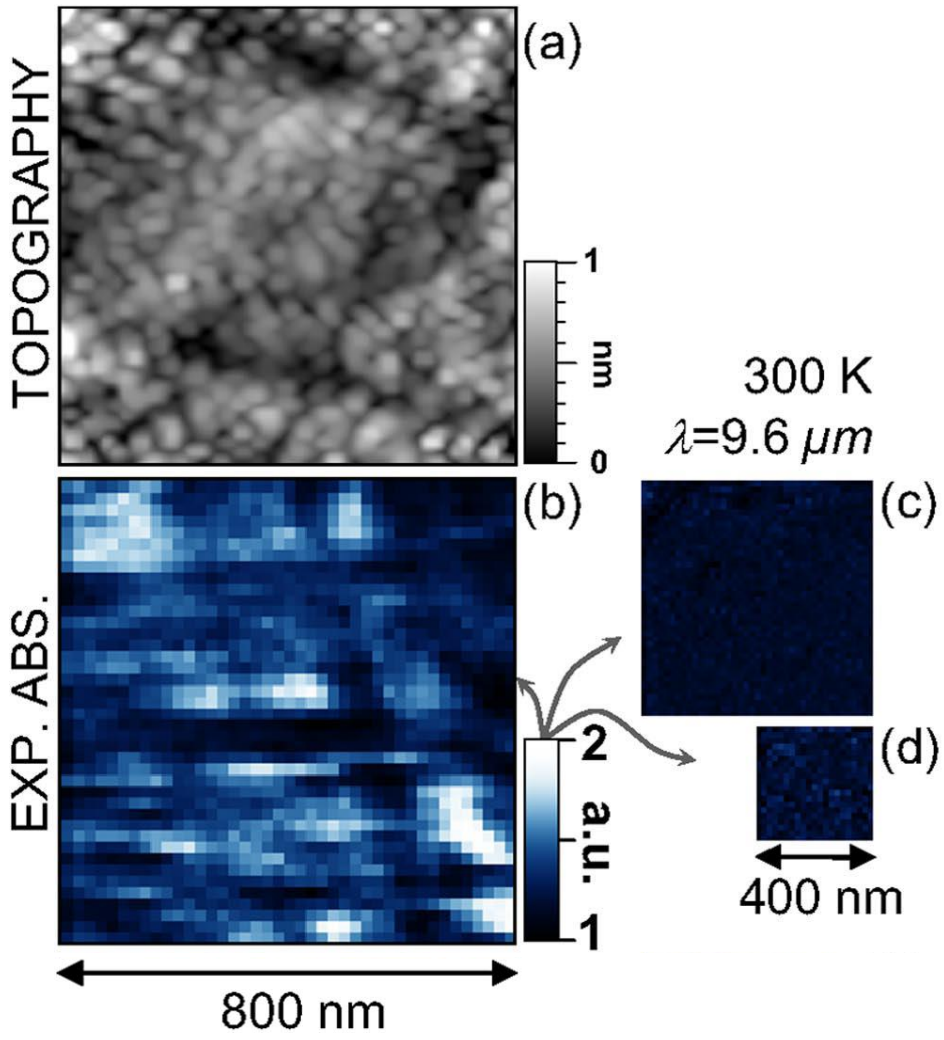

Fig 4. Study of quantum dots, a) AFM topography image of the quantum dot sample, b) corresponding AFMIR image of a quantum dot sample with nominal modulation doping of 4×10^{11} cm^{-2} recorded at 9.6 mm noting that the quantum dots appear with a bright color. c) and d) AFMIR images on two other quantum dot samples with nominal modulation doping of 4×10^{10} cm^{-2} and of 4×10^{12} cm^{-2} respectively [taken from ref 33, copyright American Physical Society, reproduced with permission].

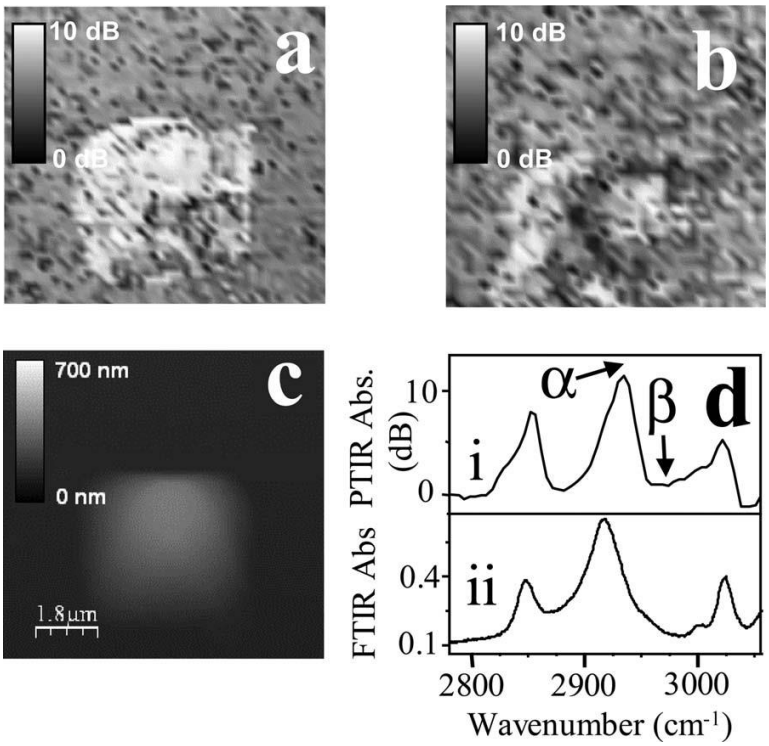

Fig. 5. Study of Polystyrene, a), Topography AFM image, b), On-resonance absorption image. c), Off-resonance absorption image. d), Spectra showing (i) AFMIR response (ii) and FTIR response of polystyrene to IR. [taken from ref 29, copyright Optical Society of America, reproduced with permission]